




Development of the trypanosomatid *Phytomonas vermiformis* in the vernal shieldbug *Peribalus strictus vernalis*

Alexander O. Frolov^{a,*}, Marina N. Malysheva^a, Vyacheslav Yurchenko^b,
Alexei Yu. Kostygov^{a,b,*} 

^a Zoological Institute, Russian Academy of Sciences, 199034 St. Petersburg, Russia

^b Life Science Research Centre, Faculty of Science, University of Ostrava, Ostrava 710 00, Czechia

ARTICLE INFO

Keywords:

Trypanosomatidae
Phytomonad
Life cycle
Morphology
Ultrastructure

ABSTRACT

Flagellates of the genus *Phytomonas* (Trypanosomatidae) are plant parasites, several species of which damage agriculturally important crops, yet their development in insect vectors (true bugs) remains poorly characterized. Here, we detail the life cycle of *Phytomonas vermiformis* in its hemipteran host, the vernal shieldbug *Peribalus strictus vernalis*, using transmission electron microscopy, providing the most comprehensive description of a phytomonad development to date. This species shows several distinctive features: formation of pseudocysts during traversal of the intestinal epithelium, presence of giant pseudocysts containing hundreds of promastigotes within salivary gland epitheliocytes, and extensive production of intracellular endomastigotes in the salivary glands. By integrating these findings with previously published data, we conducted a phylogeny-guided comparative analysis of developmental traits across *Phytomonas*, revealing evolutionary patterns such as independent losses of midgut proliferation and multiple modes of salivary gland colonization. The results expose major gaps in our understanding of phytomonad development, the resolution of which is crucial for uncovering the adaptations underlying dixenous parasitism in this group.

1. Introduction

The parasitic flagellates of the family Trypanosomatidae (Euglenozoa: Kinetoplastea) are widely known primarily due to their representatives causing serious diseases in humans and animals (Kostygov et al., 2021). These include the causative agents of African (*Trypanosoma brucei gambiense* and *T. b. rhodesiense*) and American (*T. cruzi*) human trypanosomiasis, pathogens of various wild and domestic animals (*T. b. brucei*, *T. b. evansi*, *T. b. equiperdum*, *T. congolense*, *T. simiae*, and *T. vivax*), as well as numerous *Leishmania* spp. that cause leishmaniasis (Lukeš et al., 2018; Stuart et al., 2008). All these parasites (except *T. brucei equiperdum*, which became secondarily monoxenous by switching to sexual transmission (Claes et al., 2005)) are dixenous, implying a complex life cycle with shuttling between hosts and vectors (Maslov et al., 2019). It is well documented that dixeny has evolved at least three times in the evolution of trypanosomatids: in trypanosomes, leishmaniae, and phytomonads (Kostygov et al., 2024; Lukeš et al., 2014).

The genus *Phytomonas* is of special interest because, in contrast to other members of the family Trypanosomatidae, it acquired ability to

live in various parts of plants, including seeds, fruits, flowers, phloem, and latex (Jaskowska et al., 2015; Kostygov et al., 2021). True bugs (Hemiptera: Heteroptera) serve as vectors of these parasites (Camargo and Wallace, 1994) or act as the sole hosts for species that reverted to monoxeny (Frolov et al., 2021). Phytomonads have been documented on all continents except Antarctica, with records from the tropics to the 60th parallel north (Jaskowska et al., 2015). Interest in this group has been driven largely by the deleterious impact that some species exert on agriculture by causing diseases in crops such as oil and coconut palms, coffee trees, and manioc (cassava) (Camargo, 1999). Genomes of four species have been sequenced, revealing peculiar traits of these flagellates, including substantial streamlining, heme-independent metabolism, and the absence of respiratory complexes III and IV (Butler et al., 2017; Kořený et al., 2010; Porcel et al., 2014).

However, information on the biology of phytomonads remains limited. Throughout the 20th century, they were studied predominantly as plant parasites, with little effort devoted to identifying their bug hosts and even less to studying their interactions (Camargo et al., 1990; Camargo and Wallace, 1994; Dollet, 1984; Freymuller et al., 1990;

* Corresponding authors.

E-mail addresses: frolal@yandex.ru (A.O. Frolov), kostygov@gmail.com (A.Yu. Kostygov).

<https://doi.org/10.1016/j.jip.2026.108638>

Received 26 January 2026; Received in revised form 16 April 2026; Accepted 23 April 2026

Available online 25 April 2026

0022-2011/© 2026 The Authors. Published by Elsevier Inc. This is an open access article under the CC BY license (<http://creativecommons.org/licenses/by/4.0/>).

Hanson et al., 1966; Jankevicius et al., 1989). Conversely, in the 21st century, most studies focused on barcoding the diversity of phytomonads in insects leaving aside the specificity of detected infections or identity of plant hosts (Králová et al., 2019; Maslov et al., 2007; Votýpka et al., 2012; Votýpka et al., 2019; Votýpka et al., 2010; Votýpka et al., 2024; Westenberger et al., 2004). Remarkably, despite the availability of numerous laboratory cultures of *Phytomonas* spp. isolated from various plants and insects worldwide, only a handful of them have been formally described as species (Jaskowska et al., 2015; Kostygov et al., 2021).

The life cycle of phytomonads was postulated over a century ago, soon after the description of the first representative of this lineage—*Phytomonas davidi* from the latex of *Euphorbia pilulifera* (Lafont, 1909). The phytophagous bug *Nysius euphorbiae* (Lygaeidae) was identified as the vector transmitting this parasite between plants (Lafont, 1911). Notably, this phytomonad species has not been studied further, as the only culture isolated in 1976 and initially thought to contain it (McGhee and Postell, 1976) was later identified as *Herpetomonas muscarum*, a monoxenous parasite of flies (Borghesan et al., 2013). Studies on the model species *Phytomonas serpens* demonstrated that plant-to-plant transmission of phytomonads requires their complex development within the insect vector, involving the digestive tract, hemolymph, and salivary glands (Freytmuller et al., 1990; Jankevicius et al., 1989). Within the last decade partial or detailed data on the development of several other species have been published (Frolov et al., 2019; Frolov et al., 2016; Malysheva et al., 2025; Seward et al., 2017), revealing various deviations from the scheme established for *P. serpens*. These findings indicate that the development of phytomonads in various organs and tissues of hemipteran insects warrants further study and theoretical generalization.

Phytomonas vermiformis was recently described from the vernal shieldbug *Peribalus strictus vernalis* (Hemiptera: Pentatomidae) in the European part of Russia (Frolov et al., 2024). This bug is strictly phytophagous and can feed on a wide range of plants (Wachmann, 1989), but so far the endomastigotes of *P. vermiformis* were found only in inflorescence of the common nettle, *Urtica dioica*. In this work, we detail how *Phytomonas vermiformis* develops in its hemipteran host (vector) and compare this process with that in other investigated phytomonads.

2. Materials and methods

2.1. Sampling and identification

During a previous study, eleven individuals of the vernal shieldbug *P. strictus vernalis* collected in village Oksochi, Novgorod oblast, Russia (58°39' N; 32°47' E) were found infected with *Phytomonas vermiformis* (Frolov et al., 2024). Hemolymph was examined prior to dissection by collecting a drop after leg amputation, and Giemsa-stained smears were prepared when parasites were detected. Salivary glands and fragments of the intestine from these individuals were sampled for light microscopy (Giemsa-stained smears), transmission electron microscopy (TEM) and molecular analyses.

Molecular identification of the samples was performed as described previously (Yurchenko et al., 2016). Briefly, genomic DNA extracted from infected organ fragments was used for the amplification of the full-length 18S rRNA gene with primers S762 and S763 (Maslov et al., 1996). The resulting amplicons were then Sanger-sequenced using a set of internal primers reported elsewhere (Gerasimov et al., 2012).

2.2. Electron microscopy

For TEM, the samples were fixed for 1h with an ice-cold mixture of 1.5% glutaraldehyde and 1.5% OsO₄ in 0.1 M cacodylate buffer (pH 7.4). After triple washing with 0.1 M cacodylate buffer containing 5% sucrose, they were post-fixed with 2% OsO₄ in 0.1 M cacodylate buffer for 30 min on ice. The samples were then dehydrated in an ascending ethanol series followed by propylene oxide and embedded in a 1:1

mixture of Epon and Araldite resins (Sigma-Aldrich/ Merck, St. Louis, USA). Ultrathin sections (70 nm) were prepared using an EM UC6 ultramicrotome (Leica Microsystems, Wetzlar, Germany), placed onto copper grids and contrasted with 2% uranyl acetate and 0.5% lead citrate aqueous solutions for 2 h and 5 min, respectively. The sections were examined using a Morgagni 268-D transmission electron microscope (FEI Company/Thermo Fisher Scientific, Hillsboro, USA) at an accelerating voltage of 80 kV.

2.3. Phylogenetic analysis

To investigate the evolutionary distribution of developmental traits in phytomonads, a phylogenetic analysis was performed using the genes for 18S rRNA, glycosomal glyceraldehyde-3-phosphate dehydrogenase (gGAPDH), and heat shock protein 83 (HSP83). The analysis focused on those species, for which at least partial information on the development in the insect host was available and nearly complete sequences for at least 18S rRNA gene were present (Table S1). In addition, three *Phytomonas* spp. and three outgroup species from the related genera *Herpetomonas* and *Lafontella*, all with published genomic data, were incorporated to provide better phylogenetic context, considering that particular gene sequences were missing for some taxa (Table S1).

The nucleotide sequences of 18S rRNA gene were aligned with MAFFT v7.526 (Katoh and Standley, 2013) using the E-INS-i algorithm. For the two protein-coding genes, alignments were generated in MAFFT after translating the sequences into amino acids and applying the L-INS-i method with the BLOSUM80 scoring matrix, followed by reverse translation to the original nucleotide sequences. The three alignments were concatenated and analyzed in IQ-TREE v3.0.1 (Wong et al., 2025) using a partitioning scheme (edge-proportional) and a substitution model set (F81+F+G4 / F81+F+I / TVM+F+G4 / F81+F+I / F81+F+I / HKY+F+G4 / TIM2+I+G4 for the three codon positions of each protein-coding gene and for the 18S rRNA gene), both selected under the Bayesian Information Criterion. Branch support was estimated using the standard bootstrap method with 1,000 replicates. Bayesian inference was performed on the same concatenated alignment in MrBayes v3.2.7 (Ronquist et al., 2012) following the same model set as above, with generalization of substitution models other than F81 to GTR. The optimal partitioning type (linking all branch lengths, linking them by gene, or fully unlinking) was selected based on the comparison of their marginal likelihoods estimated through stepping-stone sampling (10,000,000 generations, 1/100 sampling frequency), showing overwhelming support for the third variant ($2 \times \log BF \geq 820$). Tree inference was run with the same number of generations and sampling frequency.

3. Results

3.1. Anatomy of the host digestive system

The digestive system of the vernal shieldbug *Peribalus strictus vernalis* (Fig. 1A) includes the intestine and associated glandular appendages—salivary glands and Malpighian tubules (Fig. 1B). The overall length of the intestine reaches 16 mm, nearly twice the combined length of the thoracic and abdominal body sections (~9 mm). The thoracic part contains a short oesophagus, the M1 section of the midgut (~3.5 mm), and the adjacent salivary glands (~3 mm). The remaining midgut sections are located in the abdominal part, with the longer sections—M2 (~6.1 mm) and M4 (~2.5 mm)—arranged in a loop, and the M3 section (~1.7 mm) oriented at an angle to the central axis of the insect body (Fig. 1C). Similarly to other shieldbugs, the salivary glands of *P. strictus vernalis* have two lobes: a more massive anterior as well as a narrower and longer posterior one (Fig. 1D).

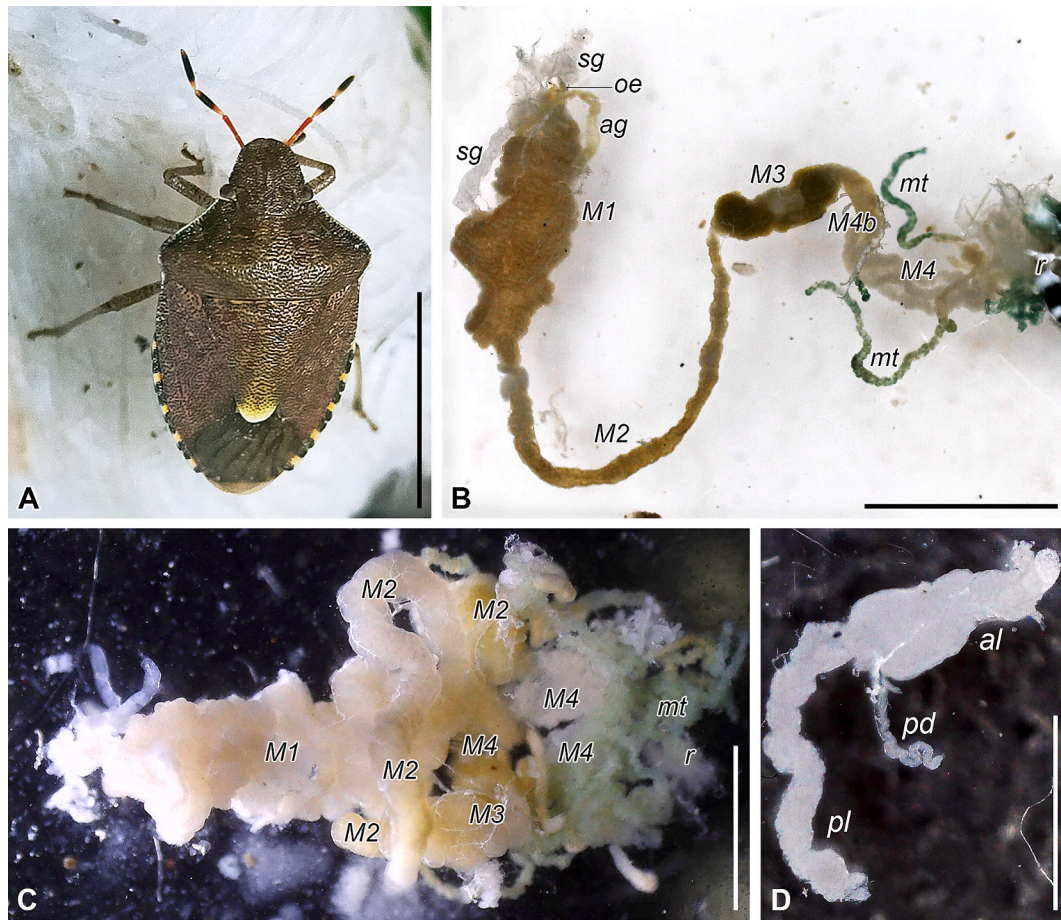


Fig. 1. Morphology and anatomy of *Peribalus strictus vernalis*. A) External appearance. B) Digestive system. C) Midgut. D) Salivary glands. Abbreviations: ag – accessory salivary gland; al – anterior lobe of the principal salivary gland; M1–M4 – midgut segments; mt – Malpighian tubules; oe – oesophagus; pd – principal duct of the salivary gland; pl – posterior lobe of the principal salivary gland; r – rectum; sg – salivary glands. Scale bars: A – 5 mm, B, C – 2 mm, D – 1 mm.

3.2. Overview of infections at the light microscopy level

Flagellates identified as *Phytomonas vermiformis* (based on 100% sequence identity by 18S rRNA gene) were found in intestine (mainly in M1–M4 midgut sections, and in lower numbers in the hindgut), hemolymph, and salivary glands of the bugs. In the gut, the parasites were predominantly represented by promastigotes of variable size with relatively long flagella (Fig. 2A, B). Occasionally, endomastigotes were observed in the anterior midgut (Fig. 2C, D). Parasites in the hemolymph were rare and consisted of exclusively giant, twisted promastigotes (Fig. 2E). The salivary glands contained clusters of intracellular promastigotes with relatively short flagella (Fig. 2F), as well as two cell types in the lumen: tadpole-like or claviform haptomonads displaying residual flagella upon detachment (Fig. 2G, H), and short, visually aflagellate endomastigotes (Fig. 2I, J).

3.3. Development in the midgut

Promastigotes of *P. vermiformis* were abundant in the midgut, both in the lumen—where they were surrounded by multimembrane structures—and in the spaces between the epithelial folds (Fig. 3A). Notably, no contacts between the parasites (either cell bodies or flagella) and the microvilli of the intestinal epithelium were detected. In the M2 section, the flagellates were also observed within enterocytes, where they localized inside parasitophorous vacuoles 10–15 µm in diameter (Fig. 3B, C). These vacuoles enclosing up to a dozen *P. vermiformis* promastigotes filled most of the volume of the infected host cells (Fig. 3B). Similar aggregations of flagellates were found on the outer

side of the midgut's M2 section (Fig. 3D), specifically in the cytoplasm of muscular and tracheolar cells, and were typically surrounded by remnants of the parasitophorous vacuole membrane (Fig. 3D).

3.4. Development in salivary glands

Outside the midgut, *P. vermiformis* promastigotes were detected in the hemolymph of infected insects, positioned close to various host organs, including the salivary glands (Figs. 4A and 5A).

The penetration of phytomonads into the salivary glands generally proceeded through the same steps as their exit from the intestinal lumen into the hemolymph, but in reverse sequence (Fig. 4B–D). The process started with the invasion of the cytoplasm of muscle cells located on the external surface of salivary glands, outwards from the basal lamina supporting the gland epithelium (Fig. 4B). These muscle cells contained clusters consisting of dozens of flagellates, lying freely, i.e. without a surrounding parasitophorous vacuole membrane. Similarly, trypanosomids infected tracheolar cells and penetrated through the basal lamina into the cytoplasm of salivary gland epitheliocytes (Fig. 4C–D). Partial destruction of the basal lamina was observed at the sites of cell aggregations (Fig. 4C).

Considering that at the initial stages of salivary gland infection phytomonads possessed free, anteriorly oriented flagella, they represented promastigotes likely capable of active flagellar motility (Fig. 4C–D). In the basal region of the epitheliocytes, individual promastigotes co-occurred with small aggregations, which apparently arose from parasite division (Fig. 4D). The advancement of phytomonads within the epithelium in the abluminal direction was accompanied by further

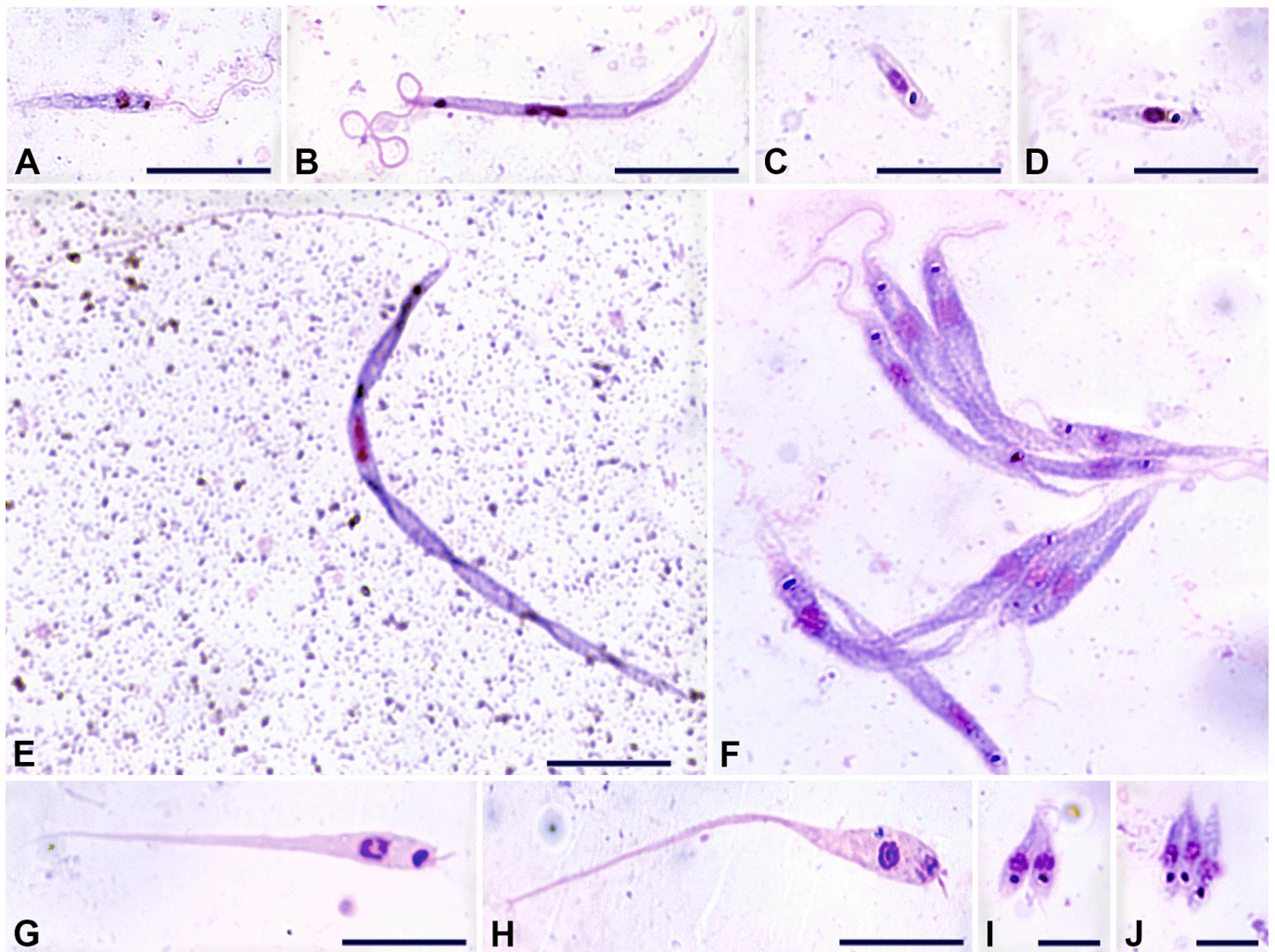


Fig. 2. Overview of life cycle stages documented by light microscopy. A, B) Promastigotes from the midgut. C, D) Endomastigotes from the anterior midgut. E) Giant promastigote from the hemolymph. F) Intracellular promastigotes from the salivary gland. G, H) Haptomonads from the salivary gland lumen. I, J) Endomastigotes from the salivary gland lumen.

differentiation. Most parasites formed giant pseudocysts: parasitophorous vacuoles containing aggregations of hundreds of cells and sometimes exceeding 50 μm in diameter (Fig. 5A-B). A smaller fraction of promastigotes transformed into endomastigotes—proliferating cells with reduced flagella and conspicuously denser cytoplasm—not surrounded by a parasitophorous vacuole membrane (Fig. 5D). In addition, individual promastigotes or small bundles similar to those detected at the initial stage of infection were also documented in the apical part of the epitheliocytes (Fig. 6A).

The exit of *P. vermiformis* into the salivary gland lumen apparently occurred through rupture of the apical surface of the host cells. This was accompanied by effusion of a translucent liquid, which enclosed the parasites and formed lacunae within the electron-dense glandular secretion (Fig. 5C-D). Such lacunae, formed at sites of massive exit of phytomonads, could merge into large areas near the epithelial surface (Fig. 5E). Two cell types could be reliably distinguished: haptomonads and endomastigotes. The former were club-shaped cells with an anteriorly located nucleus and kinetoplast, a short flagellar pocket, and a short flagellum used to attach to the brush border of the epitheliocytes by a prominent terminal bulge with several finer protrusions (Fig. 5E; 6A-B). Notably, in contrast to promastigotes, the flagella of these cells lacked a paraxonemal rod, which is likely related to their non-motility. The same was previously observed in *P. nordicus*, another species of this genus with haptomonads, for which a detailed TEM study is available

(Frolov et al., 2016). The posterior end of haptomonads was extended into thin tail filaments (Fig. 5 E).

Similar to their intracellular counterparts, endomastigotes in the gland lumen were small cells with dense cytoplasm and a flagellum that did not extend beyond the flagellar pocket (Fig. 6C-H). The axonemal microtubules were replaced by 7–9 tubular filaments, 12–14 nm in diameter (Fig. 6 G-H). In contrast to the intracellular endomastigotes, these cells exhibited markedly irregular profiles with lobe-shaped extensions, which could interlock neighboring parasites (Fig. 5E; 6E). The absence of luminal endomastigotes near the brush border suggests that they do not originate from intracellular endomastigotes but rather result from the differentiation of haptomonads.

3.5. Phylogenetic analysis

The phylogenetic tree inferred from the concatenated three-gene alignment had a topology similar to previously published reconstructions (Frolov et al., 2024; Frolov et al., 2019; Ganyukova et al., 2020; Malysheva et al., 2025; Seward et al., 2017) but showed better resolution, with high-to-maximal bootstrap supports and maximal posterior probabilities (Fig. 7). The only exception was a short branch in the crown clade encompassing species parasitic in pentatomids, likely because only one of the five species—*Phytomonas francai*—had all three gene sequences available (Table S1). This well-resolved tree was

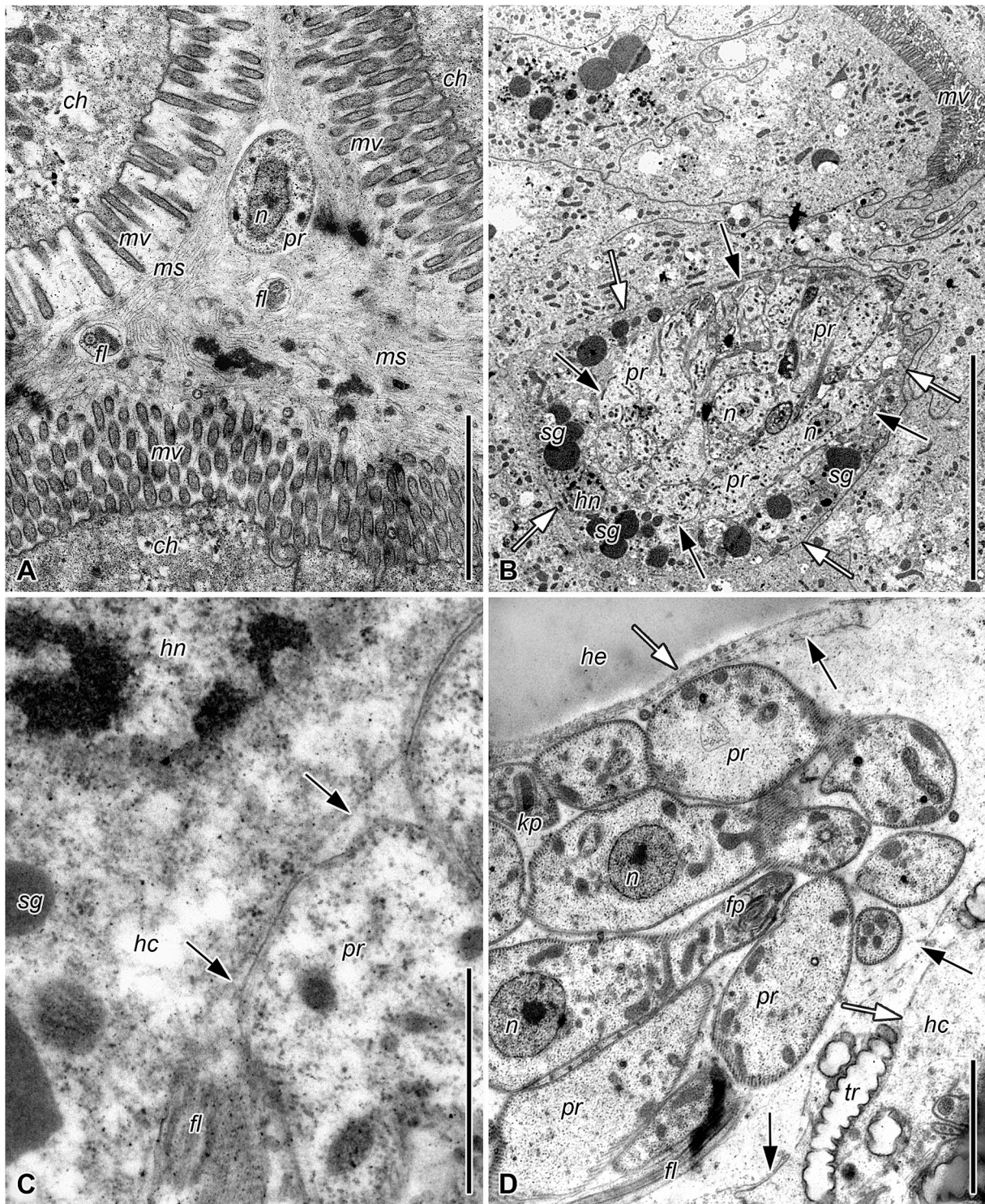


Fig. 3. *Phytomonas vermiformis* in the midgut. A) Promastigotes in the lumen. B) Promastigotes inside the parasitophorous vacuole of an enterocyte. C) Membrane of the parasitophorous vacuole. D) Promastigotes in the cytoplasm of a coelomic epitheliocyte surrounded by the degrading membrane of the parasitophorous vacuole. Abbreviations: *hc* – host cell; *fl* – flagella of promastigotes; *kp* – kinetoplast; *ms* – multimembrane structures; *mv* – microvilli; *n* – parasite nucleus; *hn* – host cell nucleus; *pr* – promastigote; *sg* – secretory granules; *tr* – tracheolar cell. White and black arrows indicate cell plasmalemma and the membrane of parasitophorous vacuole, respectively. Scale bars are: A – 2 μ m; B – 10 μ m; C – 1 μ m; D – 2 μ m.

therefore used for feature mapping to highlight evolutionary trends in the development of phytomonads within their bug hosts (see Discussion).

4. Discussion

In this work, complementing the original description of *Phytomonas vermiformis* (Frolov et al., 2024) we provide the most detailed overview of the development of a phytomonad species described to date (Fig. 8). Data available for several additional phytomonad species allowed a

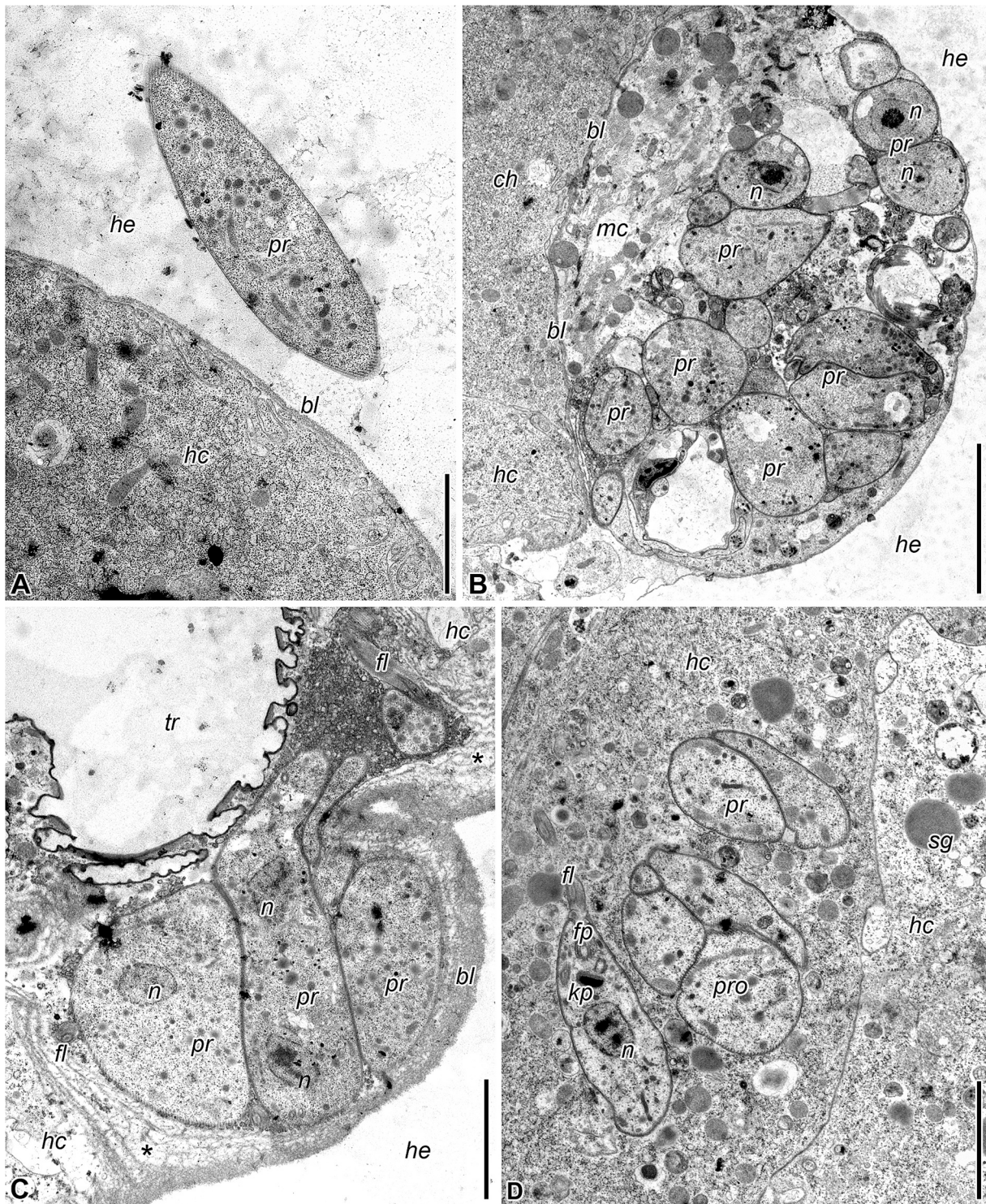


Fig. 4. Penetration of parasites into the salivary gland. A) Promastigote in the hemolymph near salivary gland. B) Promastigotes in the cytoplasm of a muscle cell at the salivary gland surface. C) Promastigotes in a tracheal cell near the basal lamina. D) Single promastigotes and small aggregates in the cytoplasm of a salivary gland epitheliocyte; note the central dividing cell with two nuclei. Abbreviations as in Fig. 2, with additions: *bl* – basal lamina; *fp* – flagellar pocket of promastigote; *he* – hemolymph. Asterisk indicates areas of basal lamina foliation. Scale bars: A – 2 μ m; B – 5 μ m; C, D – 2.5 μ m.

broader comparison, revealing both general trends and species-specific features in developmental patterns across the genus (Fig. 7).

The established hosts of the parasite under study are the vernal shieldbug *Peribalus strictus vernalis* and the common nettle *Urtica dioica* L. (Frolov et al., 2024). As in other phytomonads, *Phytomonas vermiformis* infection begins with ingestion of endomastigotes, which can be occasionally observed in the anterior midgut, but not in more posterior

intestinal regions. This suggests that endomastigotes transform into promastigotes—the major developmental stage at this site—rather than being produced there. Their presence among abundant promastigotes is more likely associated with autoinfection via saliva harboring a plethora of parasites, rather than with recent exogenous (re)infection. Although some promastigotes in the midgut lumen harbored duplicated nuclei (Frolov et al., 2024), cell division was not directly observed until the

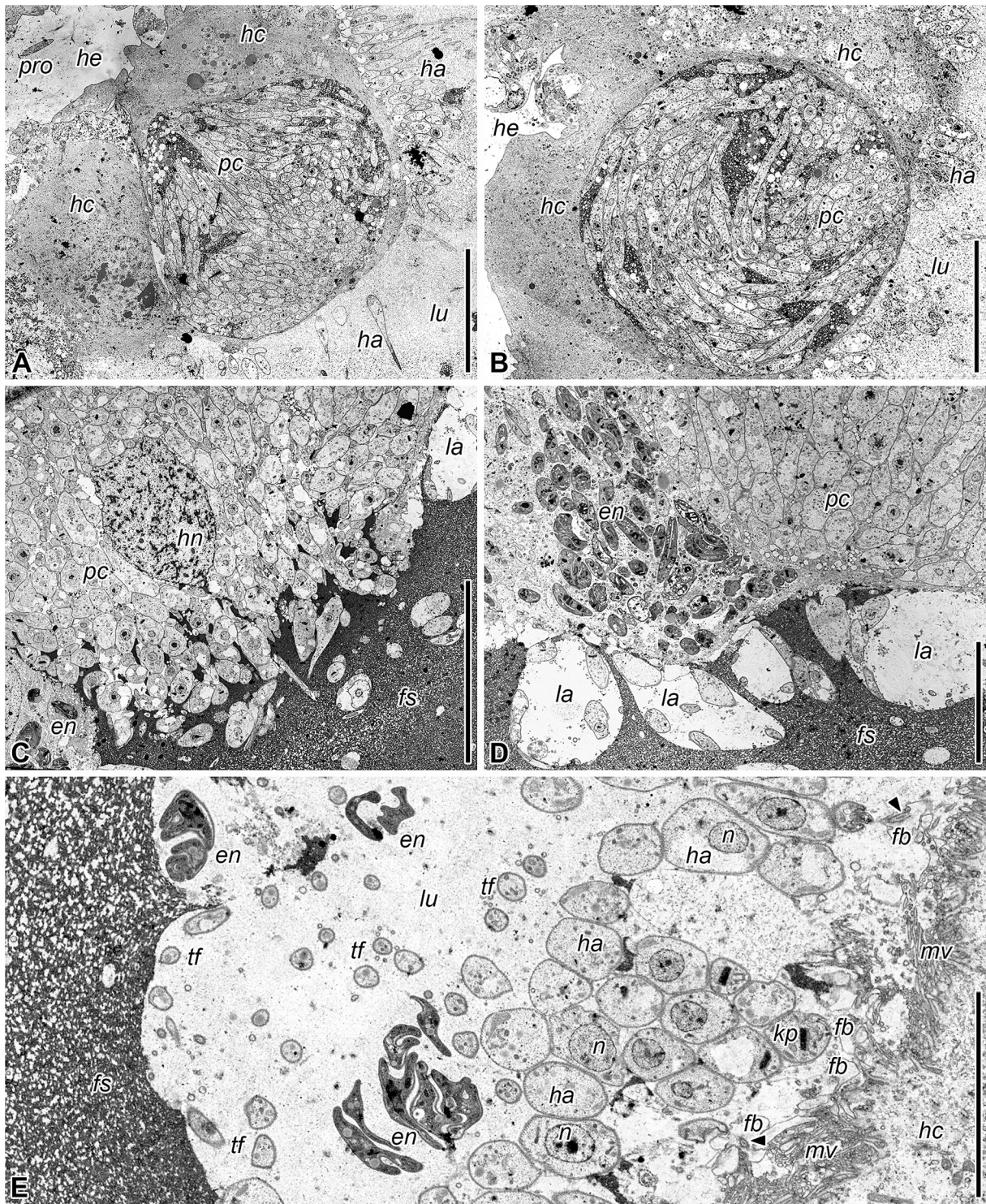


Fig. 5. Development in the salivary gland. A, B) Giant pseudocysts in epitheliocytes. C) Exit of promastigotes to the lumen, D) Intracellular and luminal stages. E) Haptomonads and endomastigotes in the lumen. Abbreviations as above, with additions: *en*, endomastigotes; *ha*, haptomonads; *la*, lacunae; *lu*, salivary gland lumen; *mv* – microvilli of epitheliocytes; *n* – nucleus of a trypanosomatid cell; *pc* – pseudocyst; *se* – salivary gland secretion; *tf* – tail filaments of a haptomonad. Scale bars: A–C – 20 μ m; D – 10 μ m; E – 5 μ m.

colonization of the midgut epithelium. In this respect, *P. vermiformis* is more similar to *P. lipae* and *P. oxycareni*, which do not divide at this location (Frolov et al., 2019; Seward et al., 2017). This contrasts with *Phytomonas nordicus* and *P. serpens*, for which proliferation in the midgut lumen was documented (Frolov and Malysheva, 1993; Frolov et al., 2016; Malysheva et al., 2023). The evolutionary distribution of this trait (Fig. 7) suggests that the last phytomonad common ancestor either

lacked proliferation in the midgut or that this ability was independently lost at least three times. Although this proliferation likely serves to maintain the intestinal micropopulation, it appears equally important for the secondary transmission route—contamination of food substrate with parasites in feces, a mechanism inherited from monoxenous trypanosomatids (Frolov et al., 2021). For this to occur, promastigotes must reach the hindgut and differentiate into endomastigotes. Both traits are

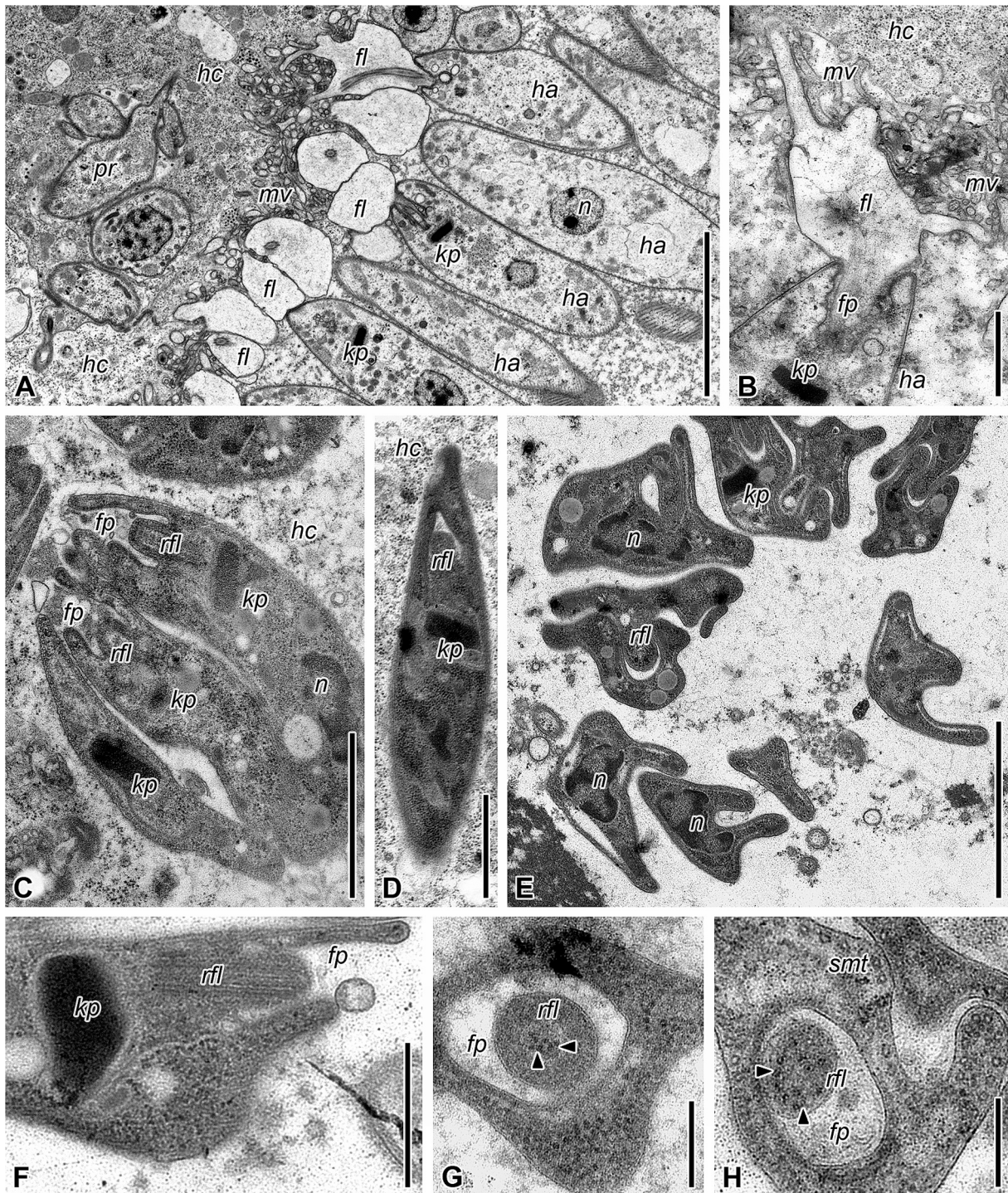


Fig. 6. Haptomonads and endomastigotes in salivary glands. A, B) Haptomonads at the brush border. C, D) Formation of endomastigotes in the cytoplasm of epitheliocytes. E) Endomastigotes in the lumen. F-H) Reduced flagellar apparatus in endomastigotes. Abbreviations as above, with additions: *rfl* – reduced flagellum; *smt* – submembrane microtubules. Arrowheads indicate residual elements of axoneme in endomastigote flagella. Scale bars: A – 4 μm ; B – 1 μm ; C – 2 μm ; D – 0.5 μm ; E – 0.25 μm .

present in *P. nordicus* and *P. serpens* (Frolov and Malysheva, 1993; Jankevicius et al., 1989), but absent in *P. lipae* and *P. oxycareni* (Frolov et al., 2019; Seward et al., 2017). The dissection method used for *P. jacuticus* did not permit determination of the localization of observed promastigotes and endomastigotes, thus not allowing to make a conclusion whether the contaminative route in this species is functional (Malysheva et al., 2025). In *P. vermiformis*, promastigotes were detected in the hindgut, while endomastigotes there were absent (Frolov et al.,

2024), suggesting a nonspecific displacement of parasites abundant in the midgut.

Penetration of *P. vermiformis* from the intestinal lumen into the epithelium results in the formation of parasitophorous vacuoles within the cytoplasm of infected enterocytes. This is partially reminiscent of the process described for *Trypanosoma rangeli* in the midgut of *Rhodnius prolixus* (Reduviidae). However, unlike that trypanosome, whose epimastigotes predominantly migrate through the cytoplasm of the

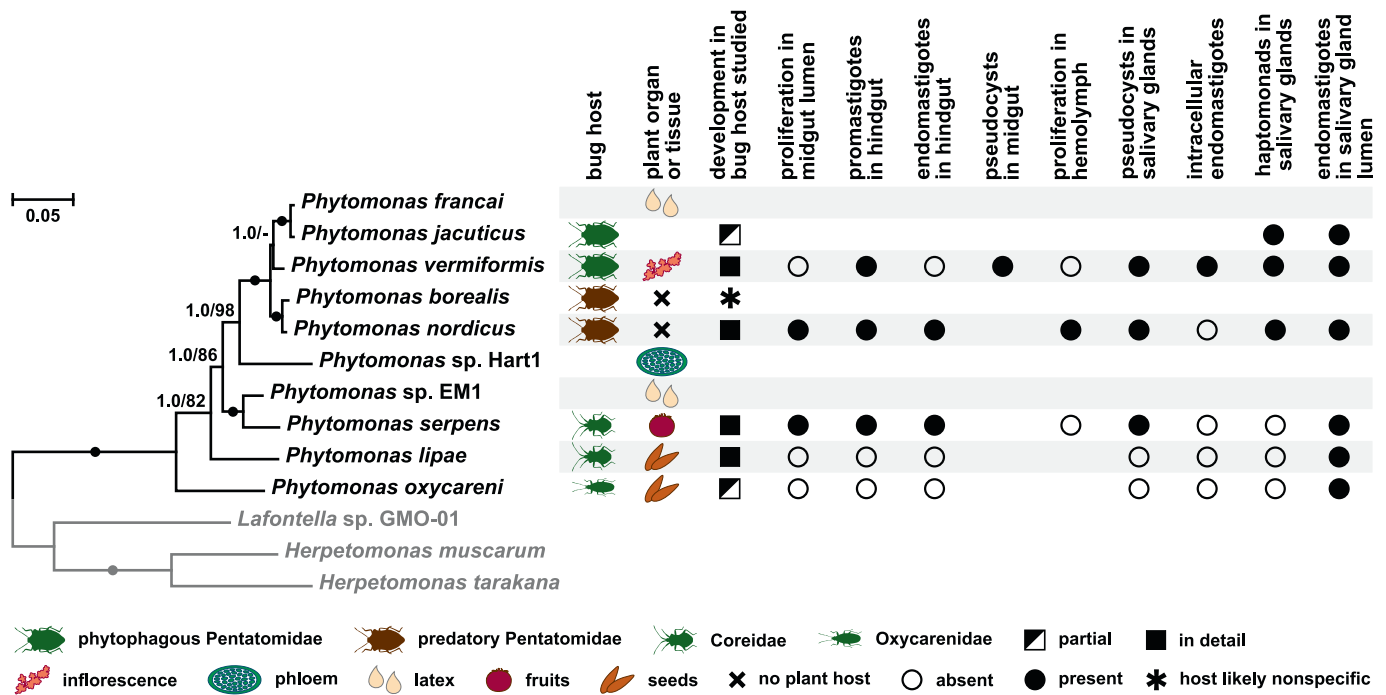


Fig. 7. Maximum likelihood phylogenetic tree of the genus *Phytomonas* based on the genes for 18S rRNA, gGAPDH, and HSP83 genes, with mapped life cycle features. Numbers on branches indicate bootstrap percentages and posterior probabilities, respectively; values below 50% are shown as dashes; absolute support by both methods is depicted by solid circles. The tree is rooted with species of the genera *Lafontella* and *Herpetomonas* (shown in grey). The scale bar represents substitutions per site. Features are explained in the graphical legend; gaps indicate missing data.

epitheliocytes in individual vacuoles (Hecker et al., 1990), *P. vermiformis* produces pseudocysts: large vacuoles containing multiple cells that occupy a substantial portion of the host cell. Both species follow the same patterns during infection of muscle and tracheolar cells; however, the fragmentation of the parasitophorous vacuole membrane was observed only in *P. vermiformis*. Traversal of the intestinal wall has not yet been investigated in other phytomonads, possibly because in those species it is a short-term and/or rare process. Notably, other trypanosomatids can exit the midgut lumen by different routes. For example, monoxenous *Blastocrithidia raabei* in the dock bug *Coreus marginatus* (Coreidae) migrates through intercellular spaces of the midgut epithelium to reach the basal lamina, beneath which the parasites accumulate. These processes, carried out by hundreds of flagellates result in a localized yet extensive perforation of the midgut wall, detachment of the basal lamina from the epithelium, and eventual degradation of the latter, causing dysfunction in this intestinal segment (Frolov et al., 2020).

Although various trypanosomatids are frequently documented in the insect's hemolymph, only for a small proportion of species (4/17, as reviewed in (Schaub, 1994)) this life stage is obligatory. Promastigotes of *P. vermiformis* were observed in the hemolymph relatively rarely (~20% of individuals) and usually in low numbers (Frolov et al., 2024). As in most other investigated *Phytomonas* spp., promastigotes in this location were never observed to divide or interact with specialized host immune cells. This contrasts with *P. nordicus* in the hemolymph of *Troilus luridus* (Pentatomidae), where promastigotes proliferate, and some are captured and lysed by hemocytes (Frolov and Malysheva, 1993). Similar events have been described for epimastigotes of *T. rangeli* in the hemolymph of *Rhodnius prolixus* (Hecker et al., 1990). Massive elimination of parasites by hemocytes was observed in an experimental infection of hemolymph by *P. serpens* (Alves e Silva et al., 2013). However, as this occurred in a nonspecific heteropteran host, *Oncopeltus fasciatus* (Lygaeidae), and involved an artificial infection method (direct injection of cultured promastigotes into the hemocoel), it is not possible to adequately compare these findings with natural processes in specific

host-parasite systems (Alves e Silva et al., 2013).

The ultimate goal of phytomonad development in insects is to reach the lumen of the salivary glands for subsequent transmission through saliva (Frolov et al., 2021). To achieve this, the flagellates traverse the gland wall, overcoming the same obstacles encountered when exiting the midgut into the hemolymph. Among phytomonads, penetration of individual parasites into the cytoplasm of host myocytes and tracheal cells has been documented previously in *P. nordicus* and *P. lipae* (Frolov et al., 2019; Frolov et al., 2016). However, unlike these two species, promastigotes of *P. vermiformis* do not merely pass through such host cells but accumulate and proliferate within them.

The modes of phytomonad traversal through the salivary gland epithelium into the lumen reveal both intra- and inter-specific differences. In *P. serpens*, naked or vacuole-enclosed single flagellates, or small aggregates, migrate through the cytoplasm of salivary gland epitheliocytes of *Phthia picta* (Coreidae), and additionally through intercellular spaces (Freymuller et al., 1990). In *P. lipae* in *C. marginatus* (Coreidae) and *P. oxycareni* in *Oxycarenum lavaterae* (Oxycarenidae), single promastigotes traverse the salivary gland epithelium within parasitophorous vacuoles (Frolov et al., 2019; Seward et al., 2017). The cells of *P. nordicus* migrating through the salivary gland epitheliocytes of *Troilus luridus* (Pentatomidae) are enclosed in parasitophorous vacuoles, where they multiply to form pseudocysts containing dozens of parasites (Frolov et al., 2016). *Phytomonas vermiformis* combines several vacuole-associated modes of epithelium traversal, ranging from single cells to giant pseudocysts containing hundreds of promastigotes.

In this study, we observed massive formation of intracellular endomastigotes within the salivary gland epitheliocytes of *P. vermiformis*, independent of their differentiation in the gland lumen. In other phytomonads, endomastigotes, the terminal developmental stage in the salivary glands adapted for the subsequent transmission to plants, are formed only in the lumen (Frolov et al., 2021). The sole exception is the detection of scarce intracellular endomastigotes in the secondary monoxenous *P. nordicus*. The role of the intracellular endomastigotes remains unclear, as their luminal counterparts are likely derived from

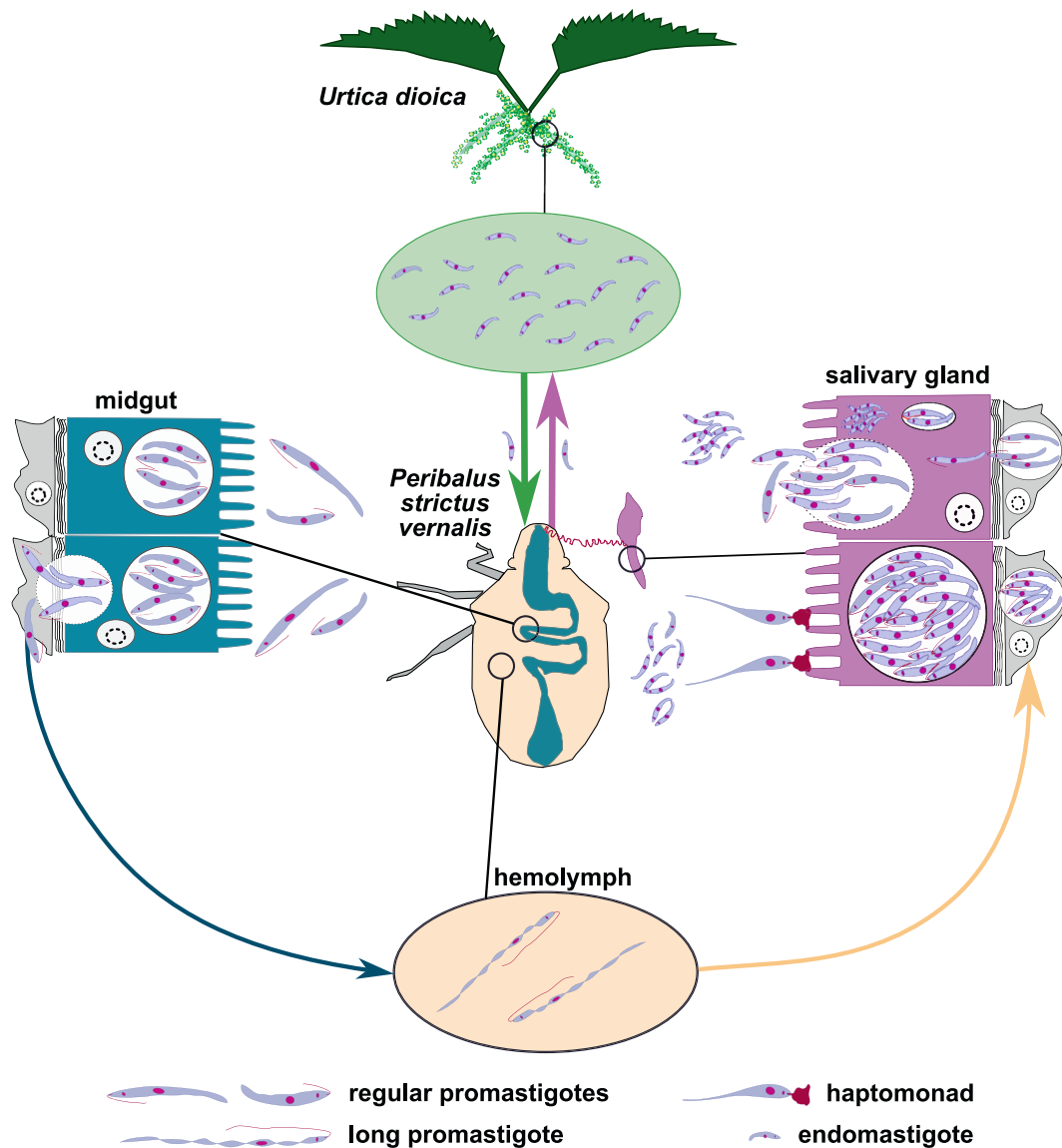


Fig. 8. Scheme of *Phytomonas vermiformis* life cycle. The information is summarized from this study and the original description of the species (Frolov et al., 2024).

haptomonads, as indicated by their relative position within the gland lumen (Fig. 5).

Notably, no free promastigotes were observed in the salivary gland lumen of *P. strictus vernalis*. Instead, there were haptomonads attached to the brush border by modified flagella. The same has been documented for *P. nordicus* and *P. jacuticus* (Frolov et al., 2016; Malysheva et al., 2025) and may represent a synapomorphy of the recently revealed Pentatomidae-parasitic phytomonad clade (Votýpka et al., 2024). In contrast, *P. lipae*, *P. serpens*, and *P. oxycareni*, which infect bugs of other families (Fig. 7) possess free promastigotes, but not haptomonads (Freytmüller et al., 1990; Frolov et al., 2019; Seward et al., 2017).

The comparative analysis presented here highlights the diversity of developmental schemes in *Phytomonas* spp., with observed similarities and differences partly reflecting adaptation to particular bug hosts, but also probably resulting from distinct evolutionary trajectories that preserve lineage-specific features. Our study provided only a preliminary overview of the phytomonad life cycles, as the data discussed reveal many knowledge gaps concerning particular parasite groups (e.g., those associated with the phloem or latex) and developmental phases (e.g., in the gut). Addressing these gaps should allow linking parasite life cycles, metabolism, and host biology.

5. Conclusions

This study provides a detailed account of *Phytomonas vermiformis* development in its insect host, revealing unique features of this parasite such as pseudocyst formation in the gut, giant salivary gland pseudocysts, and intracellular endomastigotes. Comparative analysis across *Phytomonas* spp. shows that midgut proliferation, salivary gland colonization, and endomastigote differentiation are evolutionarily flexible traits shaped by host adaptation and independent losses. These findings provide a framework for future studies on the evolution of dixenous parasitism in trypanosomatids.

CRedit authorship contribution statement

Alexander O. Frolov: Writing – original draft, Visualization, Validation, Project administration, Investigation, Formal analysis, Conceptualization. **Marina N. Malysheva:** Visualization, Investigation. **Vyacheslav Yurchenko:** Writing – review & editing, Writing – original draft. **Alexei Yu. Kostygov:** Writing – review & editing, Writing – original draft, Visualization, Validation, Methodology, Investigation, Formal analysis, Data curation.

Declaration of competing interest

The authors declare that they have no known competing financial interests or personal relationships that could have appeared to influence the work reported in this paper.

Acknowledgment

This research was supported by the State Assignments for the Zoological Institute RAS No. 125012800894-6 and 125012800903-5 as well as by the EU via the Operational Programme Just Transition and the Czech Ministry of the Environment (CZ.10.03.01/00/22_003/0000003 LERCO).

Appendix A. Supplementary data

Supplementary data to this article can be found online at <https://doi.org/10.1016/j.jip.2026.108638>.

References

- Alves e Silva, T. L., et al., 2013. The immune response of hemocytes of the insect *Oncopeltus fasciatus* against the flagellate *Phytomonas serpens*. *PLOS One*, 8, e72076. <https://doi.org/10.1371/journal.pone.0072076>.
- Borghesan, T.C., et al., 2013. Molecular phylogenetic redefinition of *Herpetomonas* (Kinetoplastea, Trypanosomatidae), a genus of insect parasites associated with flies. *Protist*, 164, 129–152. <https://doi.org/10.1016/j.protis.2012.06.001>.
- Butler, C.E., et al., 2017. Genome sequence of *Phytomonas* françai, a cassava (*Manihot esculenta*) latex parasite. *Genome Announc.* 5, e01266–01216. <https://doi.org/10.1128/genomeA.01266-16>.
- Camargo, E.P., 1999. *Phytomonas* and other trypanosomatid parasites of plants and fruit. *Adv. Parasitol.* 42, 29–112. [https://doi.org/10.1016/s0065-308x\(08\)60148-7](https://doi.org/10.1016/s0065-308x(08)60148-7).
- Camargo, E.P., et al., 1990. Trypanosomatid parasites of plants (*Phytomonas*). *Parasitol. Today*, 6, 22–25. [https://doi.org/10.1016/0169-4758\(90\)90388-k](https://doi.org/10.1016/0169-4758(90)90388-k).
- Camargo, E.P., Wallace, F.G., 1994. Vectors of plant parasites of the genus *Phytomonas* (Protozoa, Zoomastigophora, Kinetoplastida). In: Harris, K.F. (Ed.), *Adv. Dis. Vector Res.* Springer, New York, NY, pp. 333–359.
- Claes, F., et al., 2005. *Trypanosoma equiperdum*: master of disguise or historical mistake? *Trends Parasitol.* 21, 316–321. <https://doi.org/10.1016/j.pt.2005.05.010>.
- Dollet, M., 1984. Plant diseases caused by flagellate protozoa (*Phytomonas*). *Annu. Rev. Phytopathol.* 22, 115–132. <https://doi.org/10.1146/annurev.py.22.090184.000555>.
- Freytmüller, E., et al., 1990. Ultrastructural studies on the trypanosomatid *Phytomonas serpens* in the salivary glands of a phytophagous hemipteran. *J. Protozool.* 37, 225–229. <https://doi.org/10.1111/j.1550-7408.1990.tb01132.x>.
- Frolov, A.O., et al., 2024. *Phytomonas vermiformis* sp. n. (Kinetoplastea, Trypanosomatidae), a parasite of the shieldbug *Peribalus strictus vernalis* (Hemiptera, Pentatomidae). *Protistology*, 18, 89–103. <https://doi.org/10.21685/1680-0826-2024-18-2-1>.
- Frolov, A.O., et al., 2021. Development of monoxenous trypanosomatids and phytomonads in insects. *Trends Parasitol.* 37, 538–551. <https://doi.org/10.1016/j.pt.2021.02.004>.
- Frolov, A.O., Malysheva, M.N., 1993. Description of *Phytomonas nordicus* sp. n. (Trypanosomatidae) from the predatory bug *Troilus luridus* (Hemiptera, Pentatomidae). *Parazitologiya*, 27, 227–232.
- Frolov, A.O., et al., 2020. If host is refractory, insistent parasite goes berserk: Trypanosomatid *Blastocrithidia raabei* in the dock bug *Coreus marginatus*. *PLOS One*, 15, e0227832. <https://doi.org/10.1371/journal.pone.0227832>.
- Frolov, A.O., et al., 2019. Development of *Phytomonas lipae* sp. n. (Kinetoplastea: Trypanosomatidae) in the true bug *Coreus marginatus* (Heteroptera: Coreidae) and insights into the evolution of life cycles in the genus *Phytomonas*. *PLOS One*, 14, e0214484. <https://doi.org/10.1371/journal.pone.0214484>.
- Frolov, A.O., et al., 2016. Back to monoxeny: *Phytomonas nordicus* descended from dixenous plant parasites. *Eur. J. Protistol.* 52, 1–10. <https://doi.org/10.1016/j.ejop.2015.08.002>.
- Ganyukova, A.I., et al., 2020. A novel endosymbiont-containing trypanosomatid *Phytomonas borealis* sp. n. from the predatory bug *Picromerus bidens* (Heteroptera: Pentatomidae). *Folia Parasitol.* 67, 004. <https://doi.org/10.14411/fp.2020.004>.
- Gerasimov, E.S., et al., 2012. From cryptogene to gene? ND8 editing domain reduction in insect trypanosomatids. *Eur. J. Protistol.* 48, 185–193. <https://doi.org/10.1016/j.ejop.2011.09.002>.
- Hanson, W.L., et al., 1966. Experimental infection of various latex plants of family Asclepiadaceae with *Phytomonas elmsmanni*. *J. Protozool.* 13, 324–327. <https://doi.org/10.1111/j.1550-7408.1966.tb01913.x>.
- Hecker, H., et al., 1990. Development and interactions of *Trypanosoma rangeli* in and with the reduviid bug *Rhodnius prolixus*. *Parasitol. Res.* 76, 311–318. <https://doi.org/10.1007/bf00928185>.
- Jankevicius, J.V., et al., 1989. Life cycle and culturing of *Phytomonas serpens* (Gibbs), a trypanosomatid parasite of tomatoes. *J. Protozool.* 36, 265–271. <https://doi.org/10.1111/j.1550-7408.1989.tb05361.x>.
- Jaskowska, E., et al., 2015. *Phytomonas*: trypanosomatids adapted to plant environments. *PLoS Pathog.* 11, e1004484. <https://doi.org/10.1371/journal.ppat.1004484>.
- Katoh, K., Standley, D.M., 2013. MAFFT multiple sequence alignment software version 7: improvements in performance and usability. *Mol. Biol. Evol.* 30, 772–780. <https://doi.org/10.1093/molbev/mst010>.
- Korený, L., et al., 2010. Evolution of the haem synthetic pathway in kinetoplastid flagellates: an essential pathway that is not essential after all? *Int. J. Parasitol.* 40, 149–156. <https://doi.org/10.1016/j.ijpara.2009.11.007>.
- Kostygov, A.Y., et al., 2024. Phylogenetic framework to explore trait evolution in Trypanosomatidae. *Trends Parasitol.* 40, 96–99. <https://doi.org/10.1016/j.pt.2023.11.009>.
- Kostygov, A.Y., et al., 2021. Euglenozoa: taxonomy, diversity and ecology, symbioses and viruses. *Open Biol.* 11, 200407. <https://doi.org/10.1098/rsob.200407>.
- Králová, J., et al., 2019. Insect trypanosomatids in Papua New Guinea: high endemism and diversity. *Int. J. Parasitol.* 49, 1075–1086. <https://doi.org/10.1016/j.ijpara.2019.09.004>.
- Lafont, A., 1909. Sur la présence d'un parasite de la classe des flagellés dans le latex de l'Euphorbia pilulifera. *C. R. Séances Soc. Biol. Fil.* 66, 1011–1013.
- Lafont, A., 1911. Sur la transmission du *Leptomonas davidi* des euphorbes par un hémiptère, *Nysius euphorbiae*. *C. R. Séances Soc. Biol. Fil.* 70, 58–59.
- Lukeš, J., et al., 2018. Trypanosomatids are much more than just trypanosomes: clues from the expanded family tree. *Trends Parasitol.* 34, 466–480. <https://doi.org/10.1016/j.pt.2018.03.002>.
- Lukeš, J., et al., 2014. Evolution of parasitism in kinetoplastid flagellates. *Mol. Biochem. Parasitol.* 195, 115–122. <https://doi.org/10.1016/j.molbiopara.2014.05.007>.
- Malysheva, M.N., et al., 2023. Host specificity of *Phytomonas* serpens (Kinetoplastea: Trypanosomatida) to experimental vectors from two families of the true bugs, Pentatomidae and Coreidae. *Protistology*, 17, 85–91. <https://doi.org/10.21685/1680-0826-2023-17-2-3>.
- Malysheva, M.N., et al., 2025. *Phytomonas jacuticus* sp. n. (Kinetoplastea, Trypanosomatidae), a parasite of the shield bug *Carpocoris purpureipennis* (De Geer, 1773) (Hemiptera: Pentatomidae) from Yakutia. *Protistology*, 19, 200–211. <https://doi.org/10.21685/1680-0826-2025-19-3-3>.
- Maslov, D.A., et al., 1996. Phylogeny of trypanosomes as inferred from the small and large subunit rRNAs: implications for the evolution of parasitism in the trypanosomatid protozoa. *Mol. Biochem. Parasitol.* 75, 197–205. [https://doi.org/10.1016/0166-6851\(95\)02526-x](https://doi.org/10.1016/0166-6851(95)02526-x).
- Maslov, D.A., et al., 2019. Recent advances in trypanosomatid research: genome organization, expression, metabolism, taxonomy and evolution. *Parasitology*, 146, 1–27. <https://doi.org/10.1017/S0031182018000951>.
- Maslov, D.A., et al., 2007. Discovery and barcoding by analysis of spliced leader RNA gene sequences of new isolates of Trypanosomatidae from Heteroptera in Costa Rica and Ecuador. *J. Eukaryot. Microbiol.* 54, 57–65. <https://doi.org/10.1111/j.1550-7408.2006.00150.x>.
- McGhee, R.B., Postell, F.J., 1976. Axenic cultivation of *Phytomonas davidi* Lafont (Trypanosomatidae), a symbiote of laticiferous plants (Euphorbiaceae). *J. Protozool.* 23, 238–241. <https://doi.org/10.1111/j.1550-7408.1976.tb03761.x>.
- Porcel, B.M., et al., 2014. The streamlined genome of *Phytomonas* spp. relative to human pathogenic kinetoplastids reveals a parasite tailored for plants. *PLOS Genet.* 10, e1004007. <https://doi.org/10.1371/journal.pgen.1004007>.
- Ronquist, F., et al., 2012. MrBayes 3.2: efficient Bayesian phylogenetic inference and model choice across a large model space. *Syst. Biol.* 61, 539–542. <https://doi.org/10.1093/sysbio/sys029>.
- Schaub, G.A., 1994. Pathogenicity of trypanosomatids on insects. *Parasitol. Today*, 10, 463–468. [https://doi.org/10.1016/0169-4758\(94\)90155-4](https://doi.org/10.1016/0169-4758(94)90155-4).
- Seward, E.A., et al., 2017. Description of *Phytomonas oxycareni* n. sp. from the salivary glands of *Oxycareni lavatera*. *Protist*, 168, 71–79. <https://doi.org/10.1016/j.protis.2016.11.002>.
- Stuart, K., et al., 2008. Kinetoplastids: related protozoan pathogens, different diseases. *J. Clin. Invest.* 118, 1301–1310. <https://doi.org/10.1172/JCI33945>.
- Votýpka, J., et al., 2012. Cosmopolitan distribution of a trypanosomatid *Leptomonas pyrhorcoris*. *Protist*, 163, 616–631. <https://doi.org/10.1016/j.protis.2011.12.004>.
- Votýpka, J., et al., 2019. High prevalence and endemism of trypanosomatids on a small Caribbean island. *J. Eukaryot. Microbiol.* 66, 600–607. <https://doi.org/10.1111/jeu.12704>.
- Votýpka, J., et al., 2010. Probing into the diversity of trypanosomatid flagellates parasitizing insect hosts in South-West China reveals both endemism and global dispersal. *Mol. Phylogenet. Evol.* 54, 243–253. <https://doi.org/10.1016/j.ympev.2009.10.014>.
- Votýpka, J., et al., 2024. Multiple and frequent trypanosomatid co-infections of insects: the Cuban case study. *Parasitology*, 151, 567–578. <https://doi.org/10.1017/S0031182024000453>.
- Wachmann, E., 1989. *Wanzen beobachten - kennenlernen.* Neumann-Neudamm, Melsungen.
- Westenberger, S.J., et al., 2004. Trypanosomatid biodiversity in Costa Rica: genotyping of parasites from Heteroptera using the spliced leader RNA gene. *Parasitology*, 129, 537–547. <https://doi.org/10.1017/S003118200400592X>.
- Wong, T., et al., 2025. IQ-TREE 3: phylogenomic inference software using complex evolutionary models. *EcoEvoArxiv*. <https://doi.org/10.32942/x2p62n>.
- Yurchenko, V., et al., 2016. Diversity of trypanosomatids in cockroaches and the description of *Herpetomonas tarakana* sp. n. *J. Eukaryot. Microbiol.* 63, 198–209. <https://doi.org/10.1111/jeu.12268>.